



Synthesis, characterization, and photophysical properties of novel 9-phenyl-9-phosphafluorene oxide derivatives

Shuxian Qiu¹, Duan Dong², Jiahui Li¹, Huiting Wen³, Jinpeng Li¹, Yu Yang³, Shengxian Zhai^{*2} and Xingyuan Gao^{*1}

Full Research Paper

Open Access

Address:

¹College of Chemistry and Material Science, Guangdong University of Education, Guangzhou 510303, China, ²College of Chemistry and Chemical Engineering, Tarim University, Aral City 843300, China and ³College of Chemistry & Environmental Engineering, Anyang Institute of Technology, Anyang 455000, China

Email:

Shengxian Zhai^{*} - zhaishx@126.com; Xingyuan Gao^{*} - gaoxingyuan@gdei.edu.cn

* Corresponding author

Keywords:

carbazole; D–A–D type; noble-metal-free system; 9-phenyl-9-phosphafluorene oxide; photophysical properties

Beilstein J. Org. Chem. **2024**, *20*, 3299–3305.

<https://doi.org/10.3762/bjoc.20.274>

Received: 19 July 2024

Accepted: 19 December 2024

Published: 30 December 2024

Associate Editor: N. Yoshikai



© 2024 Qiu et al.; licensee Beilstein-Institut.
License and terms: see end of document.

Abstract

A novel series of D–A–D-type 9-phenyl-9-phosphafluorene oxide (PhFIOP) derivatives was prepared and is reported herein. The synthetic protocol involved 5 steps from commercially available 2-bromo-4-fluoro-1-nitrobenzene, featuring a noble-metal-free system, mild reaction conditions, and a good yield, especially for the final Cs₂CO₃-facilitated nucleophilic substitution (77–91% yield). The characterization data obtained from IR and NMR spectroscopy (¹H, ¹³C, ¹⁹F, and ³¹P) as well as HRMS spectrometry were in full agreement with the expected structures, and single-crystal X-ray diffraction analysis was conducted to confirm the structure of compound **7-H**. Moreover, the photophysical properties of these PhFIOP derivatives were determined by UV–vis absorption and photoluminescence studies, revealing that their photophysical behavior can be affected by the different substituents in the donor carbazole group.

Introduction

π -Conjugated molecular materials containing phosphine oxide (PO) groups have recently received considerable attention for their high thermal stability and unique optoelectronic features, and thus being widely applied in organic light-emitting diodes (OLEDs) [1,2]. To date, tremendous efforts have been devoted

to the development of a variety of high-performing PO-based luminescent molecules [3–21] due to the benign electron injection/transport capability of PO-containing groups. Among them, 9-phenyl-9-phosphafluorene oxide (PhFIOP) is one of the most popular core units [22–26]. Compared to the traditional PO-con-

taining moieties, PhFIOP possesses an enhanced rigid structure to reduce the possibility of nonradiative decay processes, which would improve optoelectronic properties [17,27].

Thermally activated delayed fluorescence (TADF) materials and devices have emerged rapidly in recent years, and they are mostly based on purely organic electron donor–electron acceptor (D–A) or D–A–D systems with significant intramolecular charge transfer interactions for frontier molecular orbital separation [28–30]. Due to the electron-accepting properties, PhFIOP can clearly act as an acceptor group in TADF emitters, indicating great potential for the development of highly efficient TADF molecules. In 2019, Nishida and co-workers prepared 5 D–A–D-type PhFIOP derivatives with electron-donating diarylamine or carbazole moieties in positions 2 and 8. They conducted optical and electrochemical studies, showing that the photophysical properties of PhFIOP depend on the nature of the electron-donating groups [31]. Later, Wu and co-workers introduced various electron donors to the PhFIOP unit to form new TADF emitters with high electroluminescence efficiency [32,33].

Despite this progress, TADF emitters containing the PhFIOP unit as an electron acceptor are still scarce. Meanwhile, the syntheses of the TADF emitters by the groups of Nishida and Wu both utilized palladium noble metal as a catalyst [31–33]. Therefore, it is of great significance to develop cost-effective synthetic access to PhFIOP-based TADF emitters. Additionally, the design of TADF emitters with the PhFIOP acceptor moiety and the carbazole donor moiety is lacking structural diversity. Herein, we present a 5-step synthesis of several novel D–A–D-type PhFIOP derivatives with substituted carbazole groups as donors, starting from commercially available 2-bromo-4-fluoro-

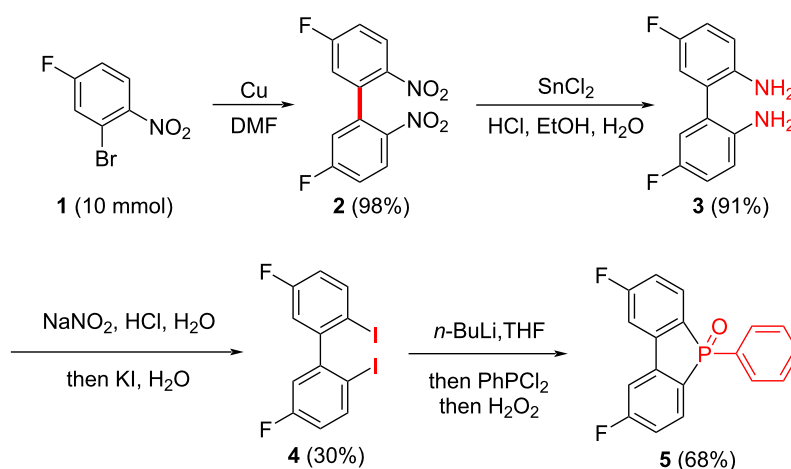
1-nitrobenzene under noble-metal-free conditions. The structures and photophysical properties of the desired molecules were also determined.

Results and Discussion

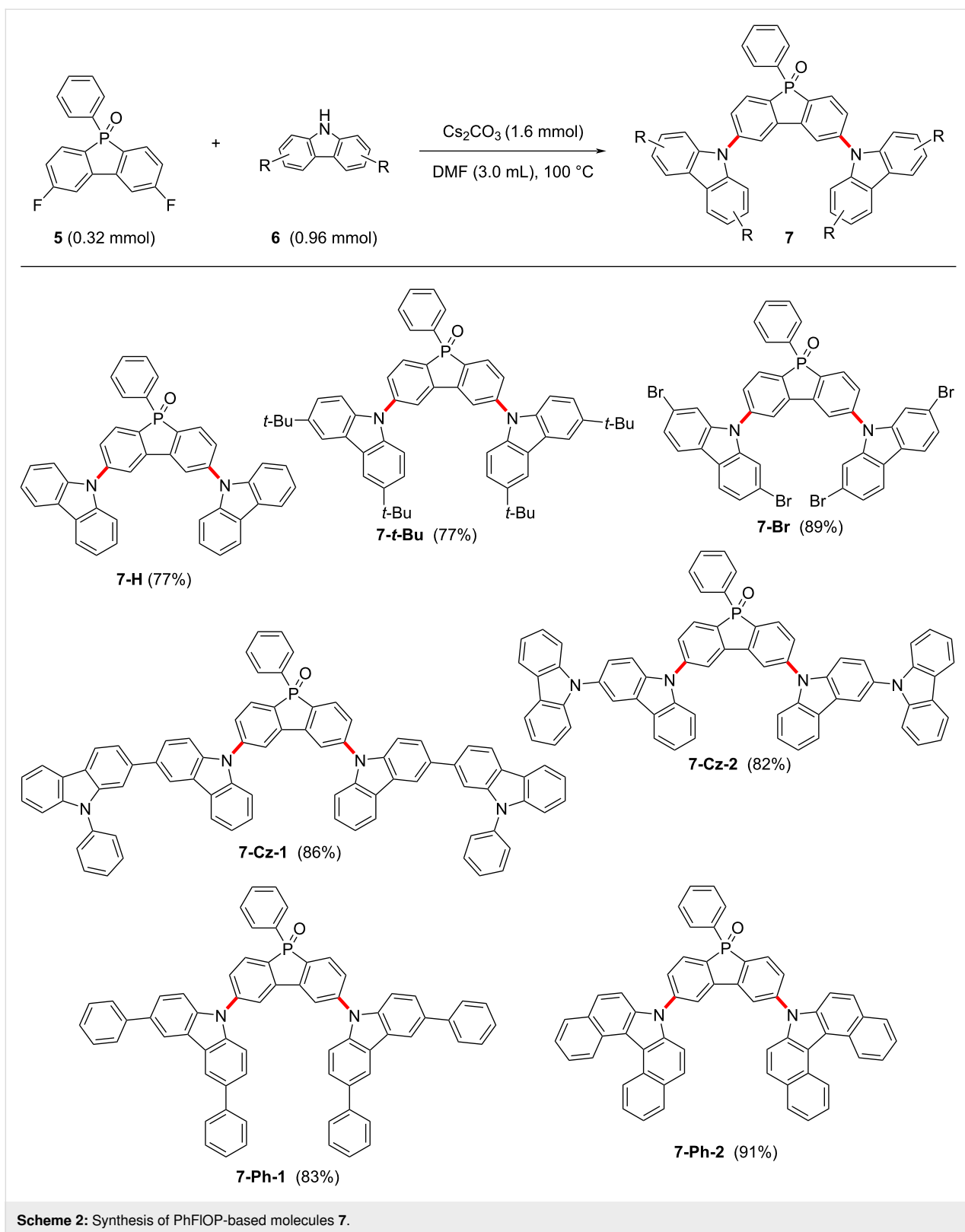
Synthesis and structural characterization

The synthesis of the PhFIOP-based compounds **7** was achieved in 5 steps starting from commercially available 2-bromo-4-fluoro-1-nitrobenzene (**1**, Scheme 1 and Scheme 2). For the preparation of the key intermediate **5** (Scheme 1), self-coupling of **1** in the presence of copper followed by reduction of the nitro group generated diamine compound **3** (89% yield over 2 steps) [34]. Upon exposure to NaNO₂/HCl, diamine **3** was transformed into a diazonium salt, which was captured by KI to deliver the diiodide **4**. Treatment of **4** with *n*-BuLi, PhPCl₂, and H₂O₂ sequentially gave 2,8-difluoro-5-phenylbenzo[*b*]phosphindole 5-oxide (**5**) in 68% yield.

With compound **5** in hand, we turned our attention to the synthesis of PhFIOP-based compounds through a Cs₂CO₃-facilitated nucleophilic substitution with substituted carbazoles as the nucleophiles (Scheme 2). For example, *tert*-butyl, bromo, carbazolyl, or phenyl substituents were introduced into the carbazoles. To our delight, by treatment of **5** with substituted carbazoles **6** in the presence of Cs₂CO₃ (5.0 equiv) in DMF at 100 °C, seven 2,8-bis(9*H*-carbazol-9-yl)-5-phenylbenzo[*b*]phosphindole 5-oxide derivatives **7** were furnished in good to excellent yields (77–91%). The structural characterization of the obtained molecules **2–7** was performed by NMR spectroscopy, which confirmed the synthetic outcomes (Figures S1–S11, Supporting Information File 1). The structures of compounds **7** were further confirmed by HRMS and IR analyses (Figures S12–S18, Supporting Information File 1).



Scheme 1: Preparation of key intermediate **5**.



In addition, the chemical structure of **7-H** was fully elucidated by single-crystal X-ray crystallography, which was performed on a Bruker APEX-II CCD diffractometer using graphite mono-

chromated Mo $K\alpha$ radiation at a temperature of 296 ± 2 K. Crystallographic data were deposited with the Cambridge Crystallographic Data Centre under accession number CCDC

2256875. The crystallographic details are summarized in Table 1, and the structure of **7-H** is shown in Figure 1 as an ORTEP diagram.

Photophysical properties

In order to investigate the photophysical properties of the PhFIOP-based molecules **7**, UV–vis absorption and photoluminescence (PL) studies were conducted. UV–vis absorption spectra of **7** in toluene solution at room temperature are shown in Figure 2, and the corresponding data are included in Table 2. The spectra in Figure 2a exhibit two major absorption bands at ≈ 290 nm and ≈ 340 nm. The band at around 290 nm might be induced by $\pi \rightarrow \pi^*$ transitions associated with the conjugated system, while the band at around 340 nm is attributed to intramolecular charge transfer processes. The low-energy absorption bands of **7-t-Bu** ($\lambda_{\max} = 345$ nm, Table 2) and **7-Cz-2** ($\lambda_{\max} = 342$ nm) are slightly redshifted compared to **7-H** ($\lambda_{\max} = 338$ nm), and larger redshifts are observed for **7-Ph-1** ($\lambda_{\max} = 354$ nm) and **7-Ph-2** ($\lambda_{\max} = 366$ nm). In contrast to **7-H**, **7-Br** ($\lambda_{\max} = 327$ nm) and **7-Cz-1** ($\lambda_{\max} = 316$ nm) show a blueshift. With a stronger electron-donating ability than **7-Cz-1**, **7-Cz-2** shows a lower energy level for the absorption band stemming from intramolecular charge transfer, as indicated by the λ_{\max} value of 342 nm. In addition, the effect of solvent polarity on the UV–vis absorption was studied with **7-H** (Figure 2b). The spectra show that there is no significant differ-

Table 1: Crystal data and structural parameters for **7-H**.

parameter	7-H
empirical formula	C ₄₂ H ₂₇ N ₂ OP
Fw	606.19
temperature (K)	296(2)
crystal system	monoclinic
space group	P2(1)/c
a (Å)	13.886(3)
b (Å)	17.477(4)
c (Å)	15.239(3)
α (deg)	90
β (deg)	105.503(4)
γ (deg)	90
volume (Å ³)	3563.7(13)
Z	4
ρ calcd (mg/m ³)	1.586
μ (Mo K α , mm ⁻¹)	0.612
F(000)	1702
number of reflections	26109
unique reflections	6289
data/restraints/parameters	8850/0/437
R_{int}	0.0253
GOF (F^2)	1.062
completeness to $\theta = 25.242$	99.8%
final R indices [$I > 2\sigma(I)$]	$R1 = 0.0769$, $wR2 = 0.2894$

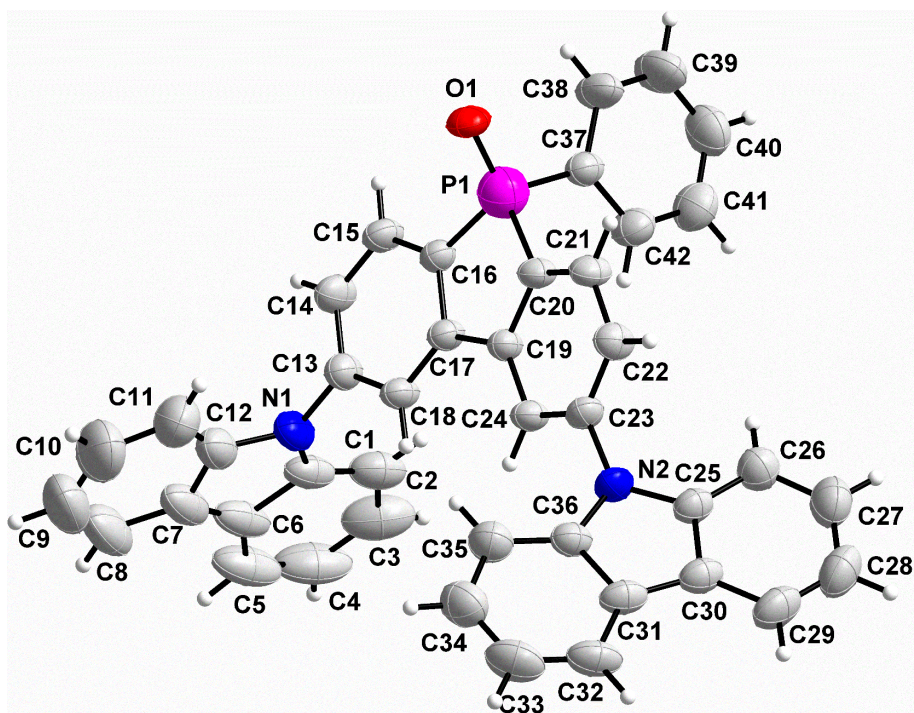


Figure 1: An ORTEP drawing obtained using the X-ray crystallographic data of **7-H**.

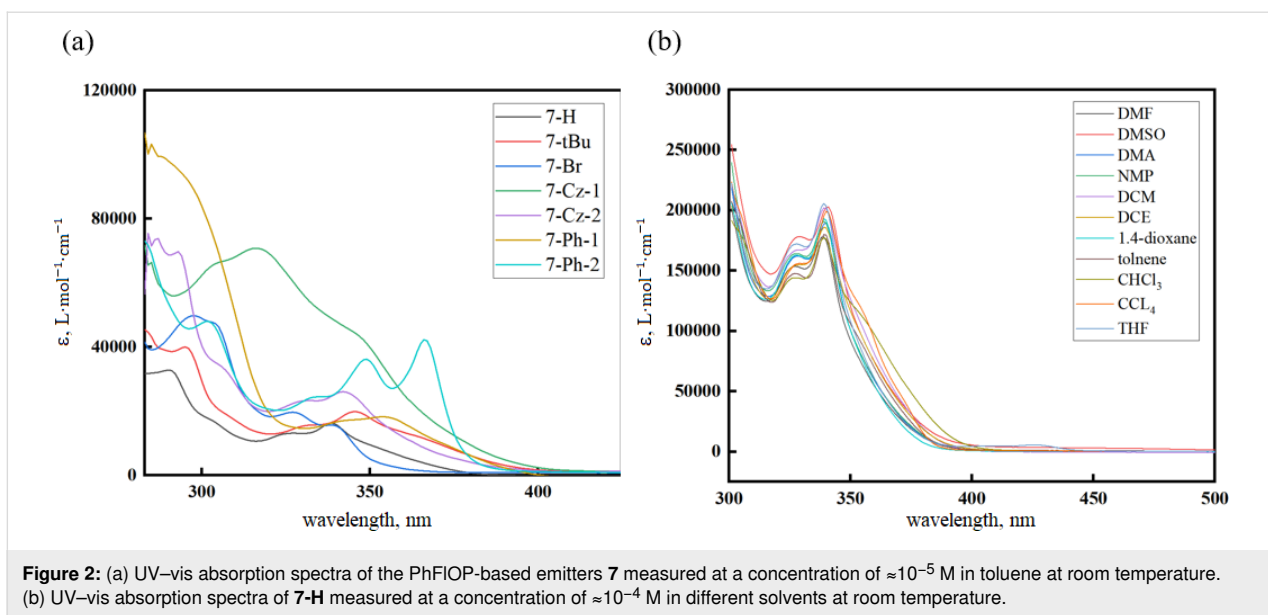


Figure 2: (a) UV-vis absorption spectra of the PhFIOP-based emitters **7** measured at a concentration of $\approx 10^{-5}$ M in toluene at room temperature. (b) UV-vis absorption spectra of **7-H** measured at a concentration of $\approx 10^{-4}$ M in different solvents at room temperature.

Table 2: Photophysical data of the PhFIOP-based emitters **7**.

compound	λ_{abs} , nm (log ϵ) ^a	λ_{em} , nm ^b	PLQY ^c	τ_{DF} (ms) ^d
7-H	290 (4.52), 338 (4.21) [291 (4.55), 338 (4.31)] ^e	408 (412, 450, 478) ^f	0.32 (0.16)	1.94 (296)
7-t-Bu	295 (4.60), 345 (4.30)	424	0.25	1.23
7-Br	298 (4.70), 327 (4.29)	383	0.22	0.88
7-Cz-1	285 (4.82), 316 (4.85)	436	0.38	1.23
7-Cz-2	293 (4.84), 342 (4.41)	444	0.31	1.15
7-Ph-1	285 (5.01), 354 (4.26)	425	0.34	1.49
7-Ph-2	302 (4.68), 349 (4.56), 366 (4.63)	392	0.27	1.17

^aMeasured at a concentration of $\approx 10^{-5}$ M in toluene at room temperature. ^bMeasured in toluene at room temperature. ^cThe absolute PL quantum yield (PLQY) was measured in degassed toluene at room temperature using an integrating sphere, and the reported PLQY of solid **7-H** is presented in parentheses [31]. ^dThe delayed fluorescence lifetime (τ_{DF}) was measured in degassed toluene at room temperature, and the reported τ_{DF} of **7-H** in toluene at 77 K is presented in parentheses [31]. ^eReported data are presented in square brackets [31]. ^fThe values in parentheses are reported λ_{em} in various solvents, namely toluene, DCM, and CH_3CN [31].

ence in the absorption bands in different solvents, indicating that the polar environment has insignificant effect on the molecular ground state of **7-H**.

The PL spectra of the PhFIOP-based compounds **7** in toluene at room temperature are shown in Figure 3, and the λ_{em} values are included in Table 2. Different emission wavelengths are observed due to the various substituents present in the donor carbazole group (Figure 3a). Compared to **7-H** ($\lambda_{\text{em}} = 408$ nm, Table 2), compounds **7-t-Bu** ($\lambda_{\text{em}} = 424$ nm), **7-Cz-1** ($\lambda_{\text{em}} = 436$ nm), **7-Cz-2** ($\lambda_{\text{em}} = 444$ nm), and **7-Ph-1** ($\lambda_{\text{em}} = 425$ nm) all show a redshift due to the electron-donating groups (*t*-Bu, Cz, Ph) on the carbazole moiety. However, **7-Ph-2** exhibits a significantly blueshifted emission maximum at 392 nm, perhaps as a consequence of a more rigid configuration. As for **7-Br**,

owing to the electron-withdrawing properties of Br, it displays a blueshifted PL maximum at 383 nm. The emission wavelength of **7-Cz-2** has a slight redshift compared to **7-Cz-1**, which may be induced by the stronger electron-donating feature of the carbazole substituent located on the donor carbazole group. In addition, we tested the emission wavelength of **7-H** in different solvents (Figure 3b) and found that the maximum is redshifted gradually with increasing solvent polarity, which indicates the CT feature in the excited state. Further, the solvent dependence of **7-H** exhibits good consistency with that reported by the Nishida group [31]. The PLQY and τ_{DF} values of the PhFIOP-based emitters **7** were measured in degassed toluene, and the corresponding data are included in Table 2, showing a PLQY ranging from 0.22–0.38 and a τ_{DF} in the order of milliseconds.

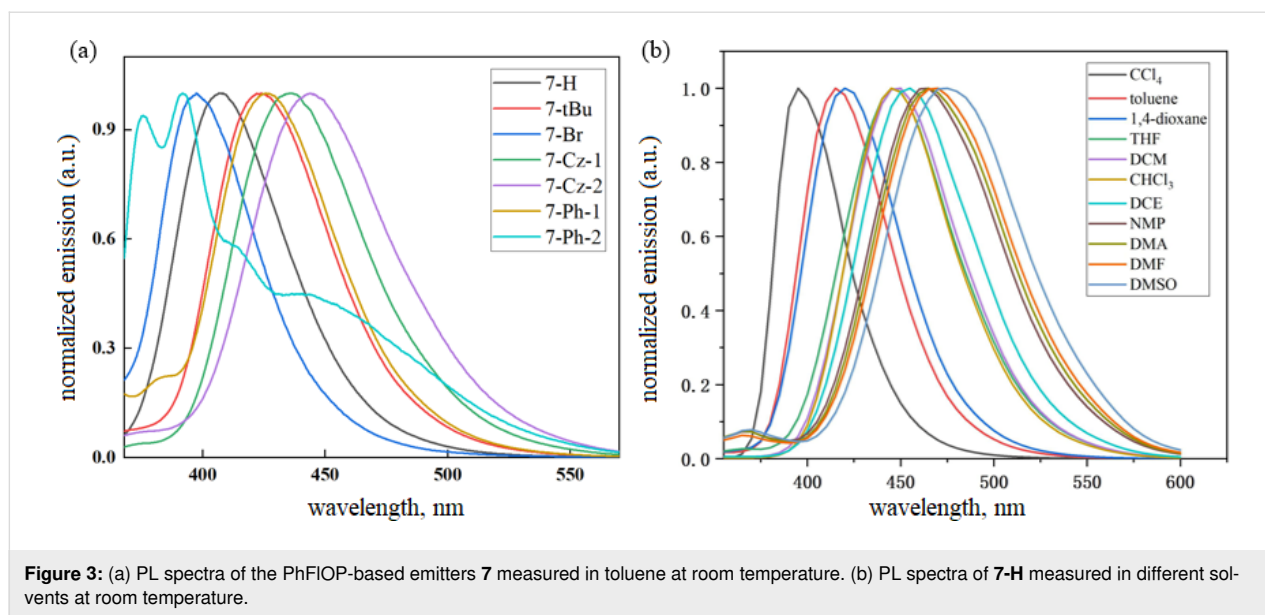


Figure 3: (a) PL spectra of the PhFIOP-based emitters **7** measured in toluene at room temperature. (b) PL spectra of **7-H** measured in different solvents at room temperature.

Conclusion

In summary, we have developed a 5-step synthesis of a series of D–A–D-type PhFIOP derivatives **7** with 2-bromo-4-fluoro-1-nitrobenzene as the starting material. This novel protocol is mild, noble-metal-free, and operationally simple. The structure of **7-H** was confirmed by single-crystal X-ray diffraction. Furthermore, UV–vis absorption and PL studies were carried out to explore the photophysical properties of these PhFIOP derivatives. Investigations for further applications of the PhFIOP-based emitters **7** are still ongoing.

XQSYS-2222873), and Guangdong Provincial Department of Education Key Area Special Project (2022ZDZX4037, 2024ZDZX2087, 2024ZDZX4063).

ORCID® iDs

Shengxian Zhai - <https://orcid.org/0000-0002-2016-1034>

Data Availability Statement

All data that supports the findings of this study is available in the published article and/or the supporting information of this article.

Supporting Information

Supporting Information File 1

General information, experimental procedures, characterization data, and copies of spectra.

[<https://www.beilstein-journals.org/bjoc/content/supplementary/1860-5397-20-274-S1.pdf>]

Acknowledgements

We are grateful to Dr. Weijian Ye of JNU for enlightening discussions.

Funding

This research was funded by the Youth Innovation Talents Project of Guangdong Universities (natural science) in China (No. 2022KQNCX052), Research and Innovation Team for Wastewater Treatment and Monitoring of Guangdong University of Education (No. 2024KYCXTD016), the quality and reform project of Guangdong province undergraduate teaching (No.

References

- Song, X.; Xu, H. *J. Inf. Disp.* **2020**, *21*, 149–172. doi:10.1080/15980316.2020.1788657
- Yoshimura, A.; Misaki, Y. *Chem. Rec.* **2021**, *21*, 3520–3531. doi:10.1002/tcr.202100107
- Su, H.-C.; Fadhel, O.; Yang, C.-J.; Cho, T.-Y.; Fave, C.; Hissler, M.; Wu, C.-C.; Réau, R. *J. Am. Chem. Soc.* **2006**, *128*, 983–995. doi:10.1021/ja0567182
- Yamaguchi, E.; Wang, C.; Fukazawa, A.; Taki, M.; Sato, Y.; Sasaki, T.; Ueda, M.; Sasaki, N.; Higashiyama, T.; Yamaguchi, S. *Angew. Chem., Int. Ed.* **2015**, *54*, 4539–4543. doi:10.1002/anie.201500229
- Wang, B.; Lv, X.; Pan, B.; Tan, J.; Jin, J.; Wang, L. *J. Mater. Chem. C* **2015**, *3*, 11192–11201. doi:10.1039/c5tc02413g
- Lee, S. Y.; Adachi, C.; Yasuda, T. *Adv. Mater. (Weinheim, Ger.)* **2016**, *28*, 4626–4631. doi:10.1002/adma.201506391
- Duan, C.; Li, J.; Han, C.; Ding, D.; Yang, H.; Wei, Y.; Xu, H. *Chem. Mater.* **2016**, *28*, 5667–5679. doi:10.1021/acs.chemmater.6b01691
- Li, J.; Ding, D.; Wei, Y.; Zhang, J.; Xu, H. *Adv. Opt. Mater.* **2016**, *4*, 522–528. doi:10.1002/adom.201500673
- Yoshikai, N.; Santra, M.; Wu, B. *Organometallics* **2017**, *36*, 2637–2645. doi:10.1021/acs.organomet.7b00244

10. Matsumura, M.; Yamada, M.; Muranaka, A.; Kanai, M.; Kakusawa, N.; Hashizume, D.; Uchiyama, M.; Yasuie, S. *Beilstein J. Org. Chem.* **2017**, *13*, 2304–2309. doi:10.3762/bjoc.13.226
11. Guo, J.; Mao, C.; Deng, B.; Ye, L.; Yin, Y.; Gao, Y.; Tu, S. *J. Org. Chem.* **2020**, *85*, 6359–6371. doi:10.1021/acs.joc.0c00118
12. Shen, Z.; Zhu, X.; Tang, W.; Feng, X. J.; Zhao, Z.; Lu, H. *J. Mater. Chem. C* **2020**, *8*, 9401–9409. doi:10.1039/d0tc01705a
13. Ye, W.; Li, X.; Ding, B.; Wang, C.; Shrestha, M.; Ma, X.; Chen, Y.; Tian, H. *J. Org. Chem.* **2020**, *85*, 3879–3886. doi:10.1021/acs.joc.9b02847
14. Duan, K.; Wang, D.; Yang, M.; Liu, Z.; Wang, C.; Tsuboi, T.; Deng, C.; Zhang, Q. *ACS Appl. Mater. Interfaces* **2020**, *12*, 30591–30599. doi:10.1021/acsami.0c02800
15. Xu, S.; Huang, H.; Yuan, C.; Liu, F.; Ding, H.; Xiao, Q. *Org. Chem. Front.* **2021**, *8*, 1747–1755. doi:10.1039/d1qo00121c
16. Haruna, B.; Hong, W.; Mohamed, W. I.; Guo, J.; Ye, L.; Yin, Y.; Gao, Y.; Tu, S. *J. Org. Chem.* **2021**, *86*, 13092–13099. doi:10.1021/acs.joc.1c00841
17. Zhong, D.; Yu, Y.; Yue, L.; Yang, X.; Ma, L.; Zhou, G.; Wu, Z. *Chem. Eng. J.* **2021**, *413*, 127445. doi:10.1016/j.cej.2020.127445
18. Sk, B.; Thangaraj, V.; Yadav, N.; Nanda, G. P.; Das, S.; Gandeepan, P.; Zysman-Colman, E.; Rajamalli, P. *J. Mater. Chem. C* **2021**, *9*, 15583–15590. doi:10.1039/d1tc03849d
19. Zhu, J.; Wei, D.; Wang, L.; Duan, Z. *J. Org. Chem.* **2022**, *87*, 11478–11490. doi:10.1021/acs.joc.2c01078
20. Zhong, D.; Yang, X.; Deng, X.; Chen, X.; Sun, Y.; Tao, P.; Li, Z.; Zhang, J.; Zhou, G.; Wong, W.-Y. *Chem. Eng. J.* **2023**, *452*, 139480. doi:10.1016/j.cej.2022.139480
21. Ledos, N.; Tondelier, D.; Geffroy, B.; Jacquemin, D.; Bouit, P.-A.; Hissler, M. *J. Mater. Chem. C* **2023**, *11*, 3826–3831. doi:10.1039/d3tc00245d
22. Geramita, K.; McBee, J.; Tilley, T. D. *J. Org. Chem.* **2009**, *74*, 820–829. doi:10.1021/jo802171t
23. Kabe, R.; Lynch, V. M.; Anzenbacher, P., Jr. *CrystEngComm* **2011**, *13*, 5423–5427. doi:10.1039/c1ce05388d
24. Xu, X.; Guo, H.; Zhao, J.; Liu, B.; Yang, X.; Zhou, G.; Wu, Z. *Chem. Mater.* **2016**, *28*, 8556–8569. doi:10.1021/acs.chemmater.6b03177
25. Mocanu, A.; Szűcs, R.; Caytan, E.; Roisnel, T.; Dorcet, V.; Bouit, P.-A.; Nyulászi, L.; Hissler, M. *J. Org. Chem.* **2019**, *84*, 957–962. doi:10.1021/acs.joc.8b02884
26. Chi, X.; Luo, L.; Wu, L.; Ren, L.; Lin, J.; Zhang, Y.; Zeng, M.-H. *J. Mol. Struct.* **2021**, *1226*, 129401. doi:10.1016/j.molstruc.2020.129401
27. Li, B.; Liu, M.; Sang, L.; Li, Z.; Wan, X.; Zhang, Y. *Adv. Opt. Mater.* **2023**, *11*, 2202610. doi:10.1002/adom.202202610
28. Yang, Z.; Mao, Z.; Xie, Z.; Zhang, Y.; Liu, S.; Zhao, J.; Xu, J.; Chi, Z.; Aldred, M. P. *Chem. Soc. Rev.* **2017**, *46*, 915–1016. doi:10.1039/c6cs00368k
29. Xie, F.-M.; Zhou, J.-X.; Li, Y.-Q.; Tang, J.-X. *J. Mater. Chem. C* **2020**, *8*, 9476–9494. doi:10.1039/d0tc02252g
30. Tenopala-Carmona, F.; Lee, O. S.; Crovini, E.; Neferu, A. M.; Murawski, C.; Olivier, Y.; Zysman-Colman, E.; Gather, M. C. *Adv. Mater. (Weinheim, Ger.)* **2021**, *33*, 2100677. doi:10.1002/adma.202100677
31. Nishida, J.-i.; Kawakami, Y.; Yamamoto, S.; Matsui, Y.; Ikeda, H.; Hirao, Y.; Kawase, T. *Eur. J. Org. Chem.* **2019**, 3735–3743. doi:10.1002/ejoc.201900189
32. Zhong, D.; Yu, Y.; Song, D.; Yang, X.; Zhang, Y.; Chen, X.; Zhou, G.; Wu, Z. *ACS Appl. Mater. Interfaces* **2019**, *11*, 27112–27124. doi:10.1021/acsami.9b05950
33. Chen, X.; Liu, S.; Sun, Y.; Zhong, D.; Feng, Z.; Yang, X.; Su, B.; Sun, Y.; Zhou, G.; Jiao, B.; Wu, Z. *Mater. Chem. Front.* **2023**, *7*, 1841–1854. doi:10.1039/d2qm01339h
34. Bhattacharjee, A.; Hosoya, H.; Ikeda, H.; Nishi, K.; Tsurugi, H.; Mashima, K. *Chem. – Eur. J.* **2018**, *24*, 11278–11282. doi:10.1002/chem.201801972

License and Terms

This is an open access article licensed under the terms of the Beilstein-Institut Open Access License Agreement (<https://www.beilstein-journals.org/bjoc/terms>), which is identical to the Creative Commons Attribution 4.0 International License (<https://creativecommons.org/licenses/by/4.0>). The reuse of material under this license requires that the author(s), source and license are credited. Third-party material in this article could be subject to other licenses (typically indicated in the credit line), and in this case, users are required to obtain permission from the license holder to reuse the material.

The definitive version of this article is the electronic one which can be found at: <https://doi.org/10.3762/bjoc.20.274>